

Search for Scalar Leptoquark Pairs Decaying to $\nu\bar{\nu}q\bar{q}$ in $p\bar{p}$ Collisions at $\sqrt{s} = 1.96$ TeV

- D. Acosta,¹⁶ J. Adelman,¹² T. Affolder,⁹ T. Akimoto,⁵⁴ M.G. Albrow,¹⁵ D. Ambrose,⁴³ S. Amerio,⁴² D. Amidei,³³ A. Anastassov,⁵⁰ K. Anikeev,¹⁵ A. Annovi,⁴⁴ J. Antos,¹ M. Aoki,⁵⁴ G. Apollinari,¹⁵ T. Arisawa,⁵⁶ J.-F. Arguin,³² A. Artikov,¹³ W. Ashmanskas,¹⁵ A. Attal,⁷ F. Azfar,⁴¹ P. Azzi-Bacchetta,⁴² N. Bacchetta,⁴² H. Bachacou,²⁸ W. Badgett,¹⁵ A. Barbaro-Galtieri,²⁸ G.J. Barker,²⁵ V.E. Barnes,⁴⁶ B.A. Barnett,²⁴ S. Baroiant,⁶ M. Barone,¹⁷ G. Bauer,³¹ F. Bedeschi,⁴⁴ S. Behari,²⁴ S. Belforte,⁵³ G. Bellettini,⁴⁴ J. Bellinger,⁵⁸ E. Ben-Haim,¹⁵ D. Benjamin,¹⁴ A. Beretvas,¹⁵ A. Bhatti,⁴⁸ M. Binkley,¹⁵ D. Bisello,⁴² M. Bishai,¹⁵ R.E. Blair,² C. Blocker,⁵ K. Bloom,³³ B. Blumenfeld,²⁴ A. Bocci,⁴⁸ A. Bodek,⁴⁷ G. Bolla,⁴⁶ A. Bolshov,³¹ P.S.L. Booth,²⁹ D. Bortoletto,⁴⁶ J. Boudreau,⁴⁵ S. Bourou,¹⁵ C. Bromberg,³⁴ E. Brubaker,¹² J. Budagov,¹³ H.S. Budd,⁴⁷ K. Burkett,¹⁵ G. Busetto,⁴² P. Bussey,¹⁹ K.L. Byrum,² S. Cabrera,¹⁴ M. Campanelli,¹⁸ M. Campbell,³³ A. Canepa,⁴⁶ M. Casarsa,⁵³ D. Carlsmith,⁵⁸ S. Carron,¹⁴ R. Carosi,⁴⁴ M. Cavalli-Sforza,³ A. Castro,⁴ P. Catastini,⁴⁴ D. Cauz,⁵³ A. Cerri,²⁸ L. Cerrito,²³ J. Chapman,³³ C. Chen,⁴³ Y.C. Chen,¹ M. Chertok,⁶ G. Chiarelli,⁴⁴ G. Chlachidze,¹³ F. Chlebana,¹⁵ I. Cho,²⁷ K. Cho,²⁷ D. Chokheli,¹³ J.P. Chou,²⁰ M.L. Chu,¹ S. Chuang,⁵⁸ J.Y. Chung,³⁸ W.-H. Chung,⁵⁸ Y.S. Chung,⁴⁷ C.I. Ciobanu,²³ M.A. Ciocci,⁴⁴ A.G. Clark,¹⁸ D. Clark,⁵ M. Coca,⁴⁷ A. Connolly,²⁸ M. Convery,⁴⁸ J. Conway,⁶ B. Cooper,³⁰ M. Cordelli,¹⁷ G. Cortiana,⁴² J. Cranshaw,⁵² J. Cuevas,¹⁰ R. Culbertson,¹⁵ C. Currat,²⁸ D. Cyr,⁵⁸ D. Dagenhart,⁵ S. Da Ronco,⁴² S. D'Auria,¹⁹ P. de Barbaro,⁴⁷ S. De Cecco,⁴⁹ G. De Lentdecker,⁴⁷ S. Dell'Agnello,¹⁷ M. Dell'Orso,⁴⁴ S. Demers,⁴⁷ L. Demortier,⁴⁸ M. Deninno,⁴ D. De Pedis,⁴⁹ P.F. Derwent,¹⁵ C. Dionisi,⁴⁹ J.R. Dittmann,¹⁵ C. Doerr,²⁵ P. Doksus,²³ A. Dominguez,²⁸ S. Donati,⁴⁴ M. Donega,¹⁸ J. Donini,⁴² M. D'Onofrio,¹⁸ T. Dorigo,⁴² V. Drollinger,³⁶ K. Ebina,⁵⁶ N. Eddy,²³ R. Ely,²⁸ R. Erbacher,⁶ M. Erdmann,²⁵ D. Errede,²³ S. Errede,²³ R. Eusebi,⁴⁷ H.-C. Fang,²⁸ S. Farrington,²⁹ I. Fedorko,⁴⁴ W.T. Fedorko,¹² R.G. Feild,⁵⁹ M. Feindt,²⁵ J.P. Fernandez,⁴⁶ C. Ferretti,³³ R.D. Field,¹⁶ G. Flanagan,³⁴ B. Flaucher,¹⁵ L.R. Flores-Castillo,⁴⁵ A. Foland,²⁰ S. Forrester,⁶ G.W. Foster,¹⁵ M. Franklin,²⁰ J.C. Freeman,²⁸ Y. Fujii,²⁶ I. Furic,¹² A. Gajjar,²⁹ A. Gallas,³⁷ J. Galyardt,¹¹ M. Gallinaro,⁴⁸ M. Garcia-Sciveres,²⁸ A.F. Garfinkel,⁴⁶ C. Gay,⁵⁹ H. Gerberich,¹⁴ D.W. Gerdes,³³ E. Gerchtein,¹¹ S. Giagu,⁴⁹ P. Giannetti,⁴⁴ A. Gibson,²⁸ K. Gibson,¹¹ C. Ginsburg,⁵⁸ K. Giolo,⁴⁶ M. Giordani,⁵³ M. Giunta,⁴⁴ G. Giurgiu,¹¹ V. Glagolev,¹³ D. Glenzinski,¹⁵ M. Gold,³⁶ N. Goldschmidt,³³ D. Goldstein,⁷ J. Goldstein,⁴¹ G. Gomez,¹⁰ G. Gomez-Ceballos,³¹ M. Goncharov,⁵¹ O. Gonzalez,⁴⁶ I. Gorelov,³⁶ A.T. Goshaw,¹⁴ Y. Gotra,⁴⁵ K. Goulianatos,⁴⁸ A. Gresele,⁴ M. Griffiths,²⁹ C. Grossos-Pilcher,¹² U. Grundler,²³ M. Guenther,⁴⁶ J. Guimaraes da Costa,²⁰ C. Haber,²⁸ K. Hahn,⁴³ S.R. Hahn,¹⁵ E. Halkiadakis,⁴⁷ A. Hamilton,³² B.-Y. Han,⁴⁷ R. Handler,⁵⁸ F. Happacher,¹⁷ K. Hara,⁵⁴ M. Hare,⁵⁵ R.F. Harr,⁵⁷ R.M. Harris,¹⁵ F. Hartmann,²⁵ K. Hatakeyama,⁴⁸ J. Hauser,⁷ C. Hays,¹⁴ H. Hayward,²⁹ E. Heider,⁵⁵ B. Heinemann,²⁹ J. Heinrich,⁴³ M. Hennecke,²⁵ M. Herndon,²⁴ C. Hill,⁹ D. Hirschbuehl,²⁵ A. Hocker,⁴⁷ K.D. Hoffman,¹² A. Holloway,²⁰ S. Hou,¹ M.A. Houlden,²⁹ B.T. Huffman,⁴¹ Y. Huang,¹⁴ R.E. Hughes,³⁸ J. Huston,³⁴ K. Ikado,⁵⁶ J. Incandela,⁹ G. Introzzi,⁴⁴ M. Iori,⁴⁹ Y. Ishizawa,⁵⁴ C. Issever,⁹ A. Ivanov,⁴⁷ Y. Iwata,²² B. Iyutin,³¹ E. James,¹⁵ D. Jang,⁵⁰ J. Jarrell,³⁶ D. Jeans,⁴⁹ H. Jensen,¹⁵ E.J. Jeon,²⁷ M. Jones,⁴⁶ K.K. Joo,²⁷ S. Jun,¹¹ T. Junk,²³ T. Kamon,⁵¹ J. Kang,³³ M. Karagoz Unel,³⁷ P.E. Karchin,⁵⁷ S. Kartal,¹⁵ Y. Kato,⁴⁰ Y. Kemp,²⁵ R. Kephart,¹⁵ U. Kerzel,²⁵ V. Khotilovich,⁵¹ B. Kilminster,³⁸ D.H. Kim,²⁷ H.S. Kim,²³ J.E. Kim,²⁷ M.J. Kim,¹¹ M.S. Kim,²⁷ S.B. Kim,²⁷ S.H. Kim,⁵⁴ T.H. Kim,³¹ Y.K. Kim,¹² B.T. King,²⁹ M. Kirby,¹⁴ L. Kirsch,⁵ S. Klimentko,¹⁶ B. Knuteson,³¹ B.R. Ko,¹⁴ H. Kobayashi,⁵⁴ P. Koehn,³⁸ D.J. Kong,²⁷ K. Kondo,⁵⁶ J. Konigsberg,¹⁶ K. Kordas,³² A. Korn,³¹ A. Korytov,¹⁶ K. Kotelnikov,³⁵ A.V. Kotwal,¹⁴ A. Kovalev,⁴³ J. Kraus,²³ I. Kravchenko,³¹ A. Kreymer,¹⁵ J. Kroll,⁴³ M. Kruse,¹⁴ V. Krutelyov,⁵¹ S.E. Kuhlmann,² N. Kuznetsova,¹⁵ A.T. Laasanen,⁴⁶ S. Lai,³² S. Lami,⁴⁸ S. Lammel,¹⁵ J. Lancaster,¹⁴ M. Lancaster,³⁰ R. Lander,⁶ K. Lannon,³⁸ A. Lath,⁵⁰ G. Latino,³⁶ R. Lauhakangas,²¹ I. Lazzizzera,⁴² Y. Le,²⁴ C. Lecci,²⁵ T. LeCompte,² J. Lee,²⁷ J. Lee,⁴⁷ S.W. Lee,⁵¹ R. Lefèvre,³ N. Leonardo,³¹ S. Leone,⁴⁴ J.D. Lewis,¹⁵ K. Li,⁵⁹ C. Lin,⁵⁹ C.S. Lin,¹⁵ M. Lindgren,¹⁵ T.M. Liss,²³ D.O. Litvintsev,¹⁵ T. Liu,¹⁵ Y. Liu,¹⁸ N.S. Lockyer,⁴³ A. Loginov,³⁵ M. Loret,⁴² P. Loverre,⁴⁹ R.-S. Lu,¹ D. Lucchesi,⁴² P. Lujan,²⁸ P. Lukens,¹⁵ G. Lungu,¹⁶ L. Lyons,⁴¹ J. Lys,²⁸ R. Lysak,¹ D. MacQueen,³² R. Madrak,²⁰ K. Maeshima,¹⁵ P. Maksimovic,²⁴ L. Malferri,⁴ G. Manca,²⁹ R. Marginean,³⁸ M. Martin,²⁴ A. Martin,⁵⁹ V. Martin,³⁷ M. Martínez,³ T. Maruyama,⁵⁴ H. Matsunaga,⁵⁴ M. Mattson,⁵⁷ P. Mazzanti,⁴ K.S. McFarland,⁴⁷ D. McGivern,³⁰ P.M. McIntyre,⁵¹ P. McNamara,⁵⁰ R. NcNulty,²⁹ S. Menzemer,³¹ A. Menzione,⁴⁴ P. Merkel,¹⁵ C. Mesropian,⁴⁸ A. Messina,⁴⁹ T. Miao,¹⁵ N. Miladinovic,⁵ L. Miller,²⁰ R. Miller,³⁴

J.S. Miller,³³ R. Miquel,²⁸ S. Miscetti,¹⁷ G. Mitselmakher,¹⁶ A. Miyamoto,²⁶ Y. Miyazaki,⁴⁰ N. Moggi,⁴
 B. Mohr,⁷ R. Moore,¹⁵ M. Morello,⁴⁴ A. Mukherjee,¹⁵ M. Mulhearn,³¹ T. Muller,²⁵ R. Mumford,²⁴ A. Munar,⁴³
 P. Murat,¹⁵ J. Nachtman,¹⁵ S. Nahn,⁵⁹ I. Nakamura,⁴³ I. Nakano,³⁹ A. Napier,⁵⁵ R. Napora,²⁴ D. Naumov,³⁶
 V. Necula,¹⁶ F. Niell,³³ J. Nielsen,²⁸ C. Nelson,¹⁵ T. Nelson,¹⁵ C. Neu,⁴³ M.S. Neubauer,⁸ C. Newman-Holmes,¹⁵
 A-S. Nicollerat,¹⁸ T. Nigmanov,⁴⁵ L. Nodulman,² O. Norniella,³ K. Oesterberg,²¹ T. Ogawa,⁵⁶ S.H. Oh,¹⁴
 Y.D. Oh,²⁷ T. Ohsugi,²² T. Okusawa,⁴⁰ R. Oldeman,⁴⁹ R. Orava,²¹ W. Orejudos,²⁸ C. Pagliarone,⁴⁴
 E. Palencia,¹⁰ R. Paoletti,⁴⁴ V. Papadimitriou,¹⁵ S. Pashapour,³² J. Patrick,¹⁵ G. Paulette,⁵³ M. Paulini,¹¹
 T. Pauly,⁴¹ C. Paus,³¹ D. Pellett,⁶ A. Penzo,⁵³ T.J. Phillips,¹⁴ G. Piacentino,⁴⁴ J. Piedra,¹⁰ K.T. Pitts,²³
 C. Plager,⁷ A. Pompoš,⁴⁶ L. Pondrom,⁵⁸ G. Pope,⁴⁵ O. Poukhov,¹³ F. Prakoshyn,¹³ T. Pratt,²⁹ A. Pronko,¹⁶
 J. Proudfoot,² F. Ptohos,¹⁷ G. Punzi,⁴⁴ J. Rademacker,⁴¹ A. Rahaman,⁴⁵ A. Rakitine,³¹ S. Rappoccio,²⁰
 F. Ratnikov,⁵⁰ H. Ray,³³ A. Reichold,⁴¹ B. Reisert,¹⁵ V. Rekovic,³⁶ P. Renton,⁴¹ M. Rescigno,⁴⁹ F. Rimondi,⁴
 K. Rinnert,²⁵ L. Ristori,⁴⁴ W.J. Robertson,¹⁴ A. Robson,⁴¹ T. Rodrigo,¹⁰ S. Rolli,⁵⁵ L. Rosenson,³¹ R. Roser,¹⁵
 R. Rossin,⁴² C. Rott,⁴⁶ J. Russ,¹¹ V. Rusu,¹² A. Ruiz,¹⁰ D. Ryan,⁵⁵ H. Saarikko,²¹ S. Sabik,³² A. Safonov,⁶
 R. St. Denis,¹⁹ W.K. Sakumoto,⁴⁷ G. Salamanna,⁴⁹ D. Saltzberg,⁷ C. Sanchez,³ A. Sansoni,¹⁷ L. Santi,⁵³
 S. Sarkar,⁴⁹ K. Sato,⁵⁴ P. Savard,³² A. Savoy-Navarro,¹⁵ P. Schlabach,¹⁵ E.E. Schmidt,¹⁵ M.P. Schmidt,⁵⁹
 M. Schmitt,³⁷ L. Scodellaro,¹⁰ A. Scribano,⁴⁴ F. Scuri,⁴⁴ A. Sedov,⁴⁶ S. Seidel,³⁶ Y. Seiya,⁴⁰ F. Semeria,⁴
 L. Sexton-Kennedy,¹⁵ I. Sfiligoi,¹⁷ M.D. Shapiro,²⁸ T. Shears,²⁹ P.F. Shepard,⁴⁵ D. Sherman,²⁰ M. Shimojima,⁵⁴
 M. Shochet,¹² Y. Shon,⁵⁸ I. Shreyber,³⁵ A. Sidoti,⁴⁴ J. Siegrist,²⁸ M. Siket,¹ A. Sill,⁵² P. Sinervo,³² A. Sisakyan,¹³
 A. Skiba,²⁵ A.J. Slaughter,¹⁵ K. Sliwa,⁵⁵ D. Smirnov,³⁶ J.R. Smith,⁶ F.D. Snider,¹⁵ R. Snihur,³² A. Soha,⁶
 S.V. Somalwar,⁵⁰ J. Spalding,¹⁵ M. Spezziga,⁵² L. Spiegel,¹⁵ F. Spinella,⁴⁴ M. Spiropulu,⁹ P. Squillacioti,⁴⁴
 H. Stadie,²⁵ B. Stelzer,³² O. Stelzer-Chilton,³² J. Strologas,³⁶ D. Stuart,⁹ A. Sukhanov,¹⁶ K. Sumorok,³¹
 H. Sun,⁵⁵ T. Suzuki,⁵⁴ A. Taffard,²³ R. Tafirout,³² S.F. Takach,⁵⁷ H. Takano,⁵⁴ R. Takashima,²² Y. Takeuchi,⁵⁴
 K. Takikawa,⁵⁴ M. Tanaka,² R. Tanaka,³⁹ N. Tanimoto,³⁹ S. Tapprogge,²¹ M. Tecchio,³³ P.K. Teng,¹ K. Terashi,⁴⁸
 R.J. Tesarek,¹⁵ S. Tether,³¹ J. Thom,¹⁵ A.S. Thompson,¹⁹ E. Thomson,⁴³ P. Tipton,⁴⁷ V. Tiwari,¹¹ S. Tkaczyk,¹⁵
 D. Toback,⁵¹ K. Tollefson,³⁴ T. Tomura,⁵⁴ D. Tonelli,⁴⁴ M. Tönnesmann,³⁴ S. Torre,⁴⁴ D. Torretta,¹⁵ S. Tourneur,¹⁵
 W. Trischuk,³² J. Tseng,⁴¹ R. Tsuchiya,⁵⁶ S. Tsuno,³⁹ D. Tsybychev,¹⁶ N. Turini,⁴⁴ M. Turner,²⁹ F. Ukegawa,⁵⁴
 T. Unverhau,¹⁹ S. Uozumi,⁵⁴ D. Usynin,⁴³ L. Vacavant,²⁸ A. Vaiciulis,⁴⁷ A. Varganov,³³ E. Vataga,⁴⁴ S. Vejcik III,¹⁵
 G. Velev,¹⁵ V. Veszpremi,⁴⁶ G. Veramendi,²³ T. Vickey,²³ R. Vidal,¹⁵ I. Vila,¹⁰ R. Vilar,¹⁰ I. Vollrath,³²
 I. Volobouev,²⁸ M. von der Mey,⁷ P. Wagner,⁵¹ R.G. Wagner,² R.L. Wagner,¹⁵ W. Wagner,²⁵ R. Wallny,⁷
 T. Walter,²⁵ T. Yamashita,³⁹ K. Yamamoto,⁴⁰ Z. Wan,⁵⁰ M.J. Wang,¹ S.M. Wang,¹⁶ A. Warburton,³² B. Ward,¹⁹
 S. Waschke,¹⁹ D. Waters,³⁰ T. Watts,⁵⁰ M. Weber,²⁸ W.C. Wester III,¹⁵ B. Whitehouse,⁵⁵ A.B. Wicklund,²
 E. Wicklund,¹⁵ H.H. Williams,⁴³ P. Wilson,¹⁵ B.L. Winer,³⁸ P. Wittich,⁴³ S. Wolbers,¹⁵ M. Wolter,⁵⁵
 M. Worcester,⁷ S. Worm,⁵⁰ T. Wright,³³ X. Wu,¹⁸ F. Würthwein,⁸ A. Wyatt,³⁰ A. Yagil,¹⁵ U.K. Yang,¹²
 W. Yao,²⁸ G.P. Yeh,¹⁵ K. Yi,²⁴ J. Yoh,¹⁵ P. Yoon,⁴⁷ K. Yorita,⁵⁶ T. Yoshida,⁴⁰ I. Yu,²⁷ S. Yu,⁴³ Z. Yu,⁵⁹
 J.C. Yun,¹⁵ L. Zanello,⁴⁹ A. Zanetti,⁵³ I. Zaw,²⁰ F. Zetti,⁴⁴ J. Zhou,⁵⁰ A. Zsenei,¹⁸ and S. Zucchelli,⁴

(CDF Collaboration)

¹ Institute of Physics, Academia Sinica, Taipei, Taiwan 11529, Republic of China² Argonne National Laboratory, Argonne, Illinois 60439³ Institut de Fisica d'Altes Energies, Universitat Autonoma de Barcelona, E-08193, Bellaterra (Barcelona), Spain⁴ Istituto Nazionale di Fisica Nucleare, University of Bologna, I-40127 Bologna, Italy⁵ Brandeis University, Waltham, Massachusetts 02254⁶ University of California at Davis, Davis, California 95616⁷ University of California at Los Angeles, Los Angeles, California 90024⁸ University of California at San Diego, La Jolla, California 92093⁹ University of California at Santa Barbara, Santa Barbara, California 93106¹⁰ Instituto de Fisica de Cantabria, CSIC-University of Cantabria, 39005 Santander, Spain¹¹ Carnegie Mellon University, Pittsburgh, PA 15213¹² Enrico Fermi Institute, University of Chicago, Chicago, Illinois 60637¹³ Joint Institute for Nuclear Research, RU-141980 Dubna, Russia¹⁴ Duke University, Durham, North Carolina 27708¹⁵ Fermi National Accelerator Laboratory, Batavia, Illinois 60510¹⁶ University of Florida, Gainesville, Florida 32611¹⁷ Laboratori Nazionali di Frascati, Istituto Nazionale di Fisica Nucleare, I-00044 Frascati, Italy

- ¹⁸ University of Geneva, CH-1211 Geneva 4, Switzerland
¹⁹ Glasgow University, Glasgow G12 8QQ, United Kingdom
²⁰ Harvard University, Cambridge, Massachusetts 02138
²¹ The Helsinki Group: Helsinki Institute of Physics; and Division of High Energy Physics, Department of Physical Sciences, University of Helsinki, FIN-00044, Helsinki, Finland
²² Hiroshima University, Higashi-Hiroshima 724, Japan
²³ University of Illinois, Urbana, Illinois 61801
²⁴ The Johns Hopkins University, Baltimore, Maryland 21218
²⁵ Institut für Experimentelle Kernphysik, Universität Karlsruhe, 76128 Karlsruhe, Germany
²⁶ High Energy Accelerator Research Organization (KEK), Tsukuba, Ibaraki 305, Japan
²⁷ Center for High Energy Physics: Kyungpook National University, Taegu 702-701; Seoul National University, Seoul 151-742; and SungKyunKwan University, Suwon 440-746; Korea
²⁸ Ernest Orlando Lawrence Berkeley National Laboratory, Berkeley, California 94720
²⁹ University of Liverpool, Liverpool L69 7ZE, United Kingdom
³⁰ University College London, London WC1E 6BT, United Kingdom
³¹ Massachusetts Institute of Technology, Cambridge, Massachusetts 02139
³² Institute of Particle Physics: McGill University, Montréal, Canada H3A 2T8; and University of Toronto, Toronto, Canada M5S 1A7
³³ University of Michigan, Ann Arbor, Michigan 48109
³⁴ Michigan State University, East Lansing, Michigan 48824
³⁵ Institution for Theoretical and Experimental Physics, ITEP, Moscow 117259, Russia
³⁶ University of New Mexico, Albuquerque, New Mexico 87131
³⁷ Northwestern University, Evanston, Illinois 60208
³⁸ The Ohio State University, Columbus, Ohio 43210
³⁹ Okayama University, Okayama 700-8530, Japan
⁴⁰ Osaka City University, Osaka 588, Japan
⁴¹ University of Oxford, Oxford OX1 3RH, United Kingdom
⁴² University of Padova, Istituto Nazionale di Fisica Nucleare, Sezione di Padova-Trento, I-35131 Padova, Italy
⁴³ University of Pennsylvania, Philadelphia, Pennsylvania 19104
⁴⁴ Istituto Nazionale di Fisica Nucleare, University and Scuola Normale Superiore of Pisa, I-56100 Pisa, Italy
⁴⁵ University of Pittsburgh, Pittsburgh, Pennsylvania 15260
⁴⁶ Purdue University, West Lafayette, Indiana 47907
⁴⁷ University of Rochester, Rochester, New York 14627
⁴⁸ The Rockefeller University, New York, New York 10021
⁴⁹ Istituto Nazionale di Fisica Nucleare, Sezione di Roma 1, University di Roma "La Sapienza," I-00185 Roma, Italy
⁵⁰ Rutgers University, Piscataway, New Jersey 08855
⁵¹ Texas A&M University, College Station, Texas 77843
⁵² Texas Tech University, Lubbock, Texas 79409
⁵³ Istituto Nazionale di Fisica Nucleare, University of Trieste/ Udine, Italy
⁵⁴ University of Tsukuba, Tsukuba, Ibaraki 305, Japan
⁵⁵ Tufts University, Medford, Massachusetts 02155
⁵⁶ Waseda University, Tokyo 169, Japan
⁵⁷ Wayne State University, Detroit, Michigan 48201
⁵⁸ University of Wisconsin, Madison, Wisconsin 53706
⁵⁹ Yale University, New Haven, Connecticut 06520

(Dated: June 19, 2018)

We report on a search for the pair production of scalar leptoquarks, LQ , using 191 pb^{-1} of proton-antiproton collision data recorded by the CDF experiment during Run II of the Tevatron. The leptoquarks are sought via their decay into a neutrino and quark yielding missing transverse energy and several jets of large transverse energy. No evidence for leptoquark production is observed, and limits are set on $\sigma(p\bar{p} \rightarrow LQ\bar{LQ}X \rightarrow \nu\bar{\nu}q\bar{q}X)$. Using a next-to-leading order theoretical prediction of the cross section for scalar leptoquark production, we exclude first-generation leptoquarks in the mass interval 78 to 117 GeV/ c^2 at the 95% confidence level for $\text{BR}(LQ \rightarrow \nu q) = 100\%$.

PACS numbers: 12.60.-i, 13.85.Rm, 14.80.-j

The remarkable symmetry between quarks and leptons in the standard model (SM) suggests that some more fundamental theory may exist, which allows interactions between them. Such interactions are mediated by a new type of particle, a leptoquark [1], which carries both lep-

ton and baryon number. A leptoquark is a color-triplet boson with spin 0 or 1, and has fractional electric charge. Leptoquarks are predicted in many extensions of the SM (e.g. grand unification, technicolor, and supersymmetry with R -parity violation). The Yukawa coupling of the

leptoquark to a lepton and quark and the branching ratio to a charged lepton, denoted by β , are model dependent. Usually it is assumed that leptoquarks couple to only one generation to accommodate experimental constraints on flavor-changing neutral currents [2], which allows one to classify leptoquarks as first-, second-, or third-generation. In $p\bar{p}$ collisions, leptoquarks can be produced in pairs via the strong interaction through gg fusion or $q\bar{q}$ annihilation. The production rate for scalar leptoquarks is essentially model-independent and is determined by the known QCD couplings and leptoquark mass.

We report on a search for pair production of scalar leptoquarks, with LQ decaying to νq , resulting in a jets and missing transverse energy (\cancel{E}_T) topology. We use $191 \pm 11 \text{ pb}^{-1}$ [3] of $p\bar{p}$ collision data at a center-of-mass energy of 1.96 TeV recorded by the Collider Detector at Fermilab (CDF) during the Tevatron Run II. This analysis is sensitive to leptoquarks of all three generations with $\beta \approx 0$. The previous lower mass limit of $98 \text{ GeV}/c^2$ [4] on first-generation leptoquarks in this final state was set by the DØ Collaboration. The CDF Collaboration has also published [5] lower mass limits of $123 \text{ GeV}/c^2$ and $148 \text{ GeV}/c^2$ respectively on second- and third-generation leptoquarks in the \cancel{E}_T plus heavy-flavor jets final state. Limits on leptoquark production from the Tevatron Run I and HERA experiments as of 1999 are summarized in [6].

CDF is a general-purpose detector that is described in detail elsewhere [7]. The components relevant to this analysis are briefly described here. The charged-particle tracking system is closest to the beam pipe, and consists of multi-layer silicon detectors and a large open-cell drift chamber covering the pseudorapidity [8] region $|\eta| < 1$. The tracking system is enclosed in a superconducting solenoid, which in turn is surrounded by a calorimeter. The CDF calorimeter system is organized into electromagnetic and hadronic sections segmented in projective tower geometry, and covers the region $|\eta| < 3.6$. The electromagnetic calorimeters utilize a lead-scintillator sampling technique, whereas the hadron calorimeters use iron-scintillator technology. The central muon-detection system, used for this analysis, is located outside of the calorimeter and covers the range $|\eta| < 1$.

This search centers on selecting events with large \cancel{E}_T and a pair of jets that are acollinear in the transverse plane, because of the neutrinos in the final state. The \cancel{E}_T [8] is defined as the energy imbalance in the plane transverse to the beam direction. A jet is defined as a localized energy deposition in the calorimeter and is reconstructed using a cone algorithm with fixed radius $\Delta R \equiv \sqrt{\Delta\eta^2 + \Delta\phi^2} = 0.4$ in $\eta - \phi$ space [9]. We correct [9] jet E_T measurements and \cancel{E}_T for detector effects.

The data sample for this analysis was collected using an inclusive \cancel{E}_T trigger, which is distributed across three levels of online event selection. In the first and second levels of the trigger, \cancel{E}_T is required to be greater than

25 GeV and is calculated by summing over calorimeter trigger towers [10] with transverse energies above 1 GeV. At Level-3 \cancel{E}_T is required to be greater than 45 GeV and is recalculated using full calorimeter segmentation with a tower energy threshold of 100 MeV. We use events from the inclusive high- p_T lepton (e or μ) samples to measure the trigger efficiency directly from data. To reduce systematic effects associated with the online trigger threshold, we select events offline with $\cancel{E}_T > 60 \text{ GeV}$, where the trigger is fully efficient.

The event electromagnetic fraction (F_{em}) and charged fraction (F_{ch}) [11] are used to remove events associated with beam halo and cosmic ray sources. We reject events that contain little energy in the electromagnetic section of the calorimeter or that have mostly neutral-particle jets, by requiring $F_{em} > 0.1$ and $F_{ch} > 0.1$. There are 148,462 events in our analysis sample after the initial selection.

The dominant backgrounds to the leptoquark search in the jets and \cancel{E}_T signature are QCD multi-jet production, W and Z boson production in association with one or more jets, and top quark pair production. The ALPGEN generator [12] was used for the simulation of the W and Z boson plus parton production, with HERWIG [13] used to model parton showers. We use the exclusive $Z(\rightarrow ee) + 1 \text{ jet}$ sample to determine a scale factor between data and simulation, and apply this factor to all $W/Z + \text{jets}$ simulation samples. HERWIG was also used to estimate the contribution from $t\bar{t}$ production.

Data selection requirements were chosen to maximize the statistical significance of the leptoquark signal over background events based on studies of simulated event samples before the signal region data were examined. In addition to $\cancel{E}_T > 60 \text{ GeV}$, the signal region is defined by requiring that the two highest E_T jets ($E_T^{j_1} > 40 \text{ GeV}$, $E_T^{j_2} > 25 \text{ GeV}$) be in the central region $|\eta| < 1$. A third jet with $E_T > 15 \text{ GeV}$ and $|\eta| < 2.5$ is allowed, and we veto events with any additional jets with $E_T > 15 \text{ GeV}$ and $|\eta| < 3.6$. To reject events with \cancel{E}_T resulting from jet energy mismeasurement, we require that the opening angle in the transverse plane between the two highest E_T jets satisfy $80^\circ < \Delta\phi(j_1, j_2) < 165^\circ$. The \cancel{E}_T direction must not be parallel to any of the jets; we require the minimum azimuthal separation between the direction of the jets and \cancel{E}_T to satisfy $30^\circ < \min \Delta\phi(j, \cancel{E}_T) < 135^\circ$. The \cancel{E}_T also must not be antiparallel to the leading E_T jet: $100^\circ < \Delta\phi(j_1, \cancel{E}_T) < 165^\circ$. These criteria reject most of the QCD multi-jet background events. To reduce the background contribution from $W/Z + \text{jets}$ and $t\bar{t}$ production, we reject events with one or more identified leptons with $E_T > 10 \text{ GeV}$ (electron candidates) or $p_T > 10 \text{ GeV}/c$ (muon candidates). Criteria similar to those in [14] are used to identify the leptons. To further reduce this background we require each jet not to be highly electromagnetic (jet electromagnetic fraction < 0.9) and to have 4 or more associated tracks for cen-

tral jets ($|\eta| < 1$).

Two methods are employed to estimate the QCD multi-jet contribution in the signal region directly from the inclusive \cancel{E}_T data sample. Among all the offline analysis selection requirements, the azimuthal angular separation requirement between the \cancel{E}_T direction and a jet is most effective at removing QCD multi-jet events. Therefore, for the first method, in addition to the signal region we define a region which is rich in QCD multi-jet events by requiring that a jet is close to the \cancel{E}_T direction ($20^\circ < \min \Delta\phi(j, \cancel{E}_T) < 27^\circ$). Studies of simulated QCD multi-jet samples show that the shape of the \cancel{E}_T distribution in this region is similar to the \cancel{E}_T distribution in the signal region. We use \cancel{E}_T and $\min \Delta\phi(j, \cancel{E}_T)$ requirements to define four kinematic regions:

- A) $50 < \cancel{E}_T < 57$ GeV, $20^\circ < \min \Delta\phi(j, \cancel{E}_T) < 27^\circ$.
- B) $\cancel{E}_T > 60$ GeV, $20^\circ < \min \Delta\phi(j, \cancel{E}_T) < 27^\circ$.
- C) $50 < \cancel{E}_T < 57$ GeV, $30^\circ < \min \Delta\phi(j, \cancel{E}_T) < 135^\circ$.
- D) $\cancel{E}_T > 60$ GeV, $30^\circ < \min \Delta\phi(j, \cancel{E}_T) < 135^\circ$.

The regions A, B and C are used to extrapolate the QCD multi-jet contribution into the signal region D: $N_D = \frac{N_B}{N_A} N_C$, where N_A , N_B , and N_C are the remaining number of events in regions A, B, and C, after the $W/Z+jets$ and $t\bar{t}$ contributions have been subtracted. For the second method, the combined selection requirement efficiency is measured as a function of \cancel{E}_T in an independent inclusive jet sample at low \cancel{E}_T . The extrapolated results of this measurement is then applied to the inclusive \cancel{E}_T sample after the $W/Z+jets$ and $t\bar{t}$ contributions have been subtracted. We predict 15.0 ± 8.0 and 21.5 ± 12.4 multi-jet events for the first and second methods respectively. We take the weighted average and uncertainty of the two methods as our estimate of the multi-jet background.

We check the simulation predictions for $W/Z+jets$ with data in a control region, which is defined by requiring, in addition to 2 or 3 jets, $\cancel{E}_T > 60$ GeV and at least one electron or muon. We observe 144 events in our inclusive \cancel{E}_T sample, which is in excellent agreement with 154.3 ± 27.9 events predicted from SM processes.

The total detection efficiency (ϵ_{LQ_1}) for the first-generation scalar leptoquark (LQ_1) signal is estimated using the PYTHIA event generator [15], and the CDF detector simulation program. The PYTHIA underlying event simulation was tuned to reproduce CDF data [16]. The samples were generated using the CTEQ5L [17] parton distribution functions (PDF), with the renormalization and factorization scales set to $\mu = m_{LQ_1}$. Table I lists the total detection efficiency ϵ_{LQ_1} and the corresponding total fractional uncertainty δ_{tot} for various leptoquark masses. Also listed are the NLO cross sections [18] calculated for two choices of the μ scale. The systematic

TABLE I: Summary of the first-generation scalar leptoquark detection efficiency (ϵ_{LQ_1}), the relative uncertainty on detection efficiency (δ_{tot}), and the next-to-leading order cross section (σ_{NLO}) for two choices of the renormalization scale as functions of leptoquark mass.

m_{LQ_1} (GeV/ c^2)	ϵ_{LQ_1}	δ_{tot} (%)	σ_{NLO} (pb)	
			$\mu = m_{LQ_1}$	$\mu = 2m_{LQ_1}$
75	0.0073	29	69.4	58.8
80	0.0113	26	49.2	41.5
90	0.0187	23	26.0	22.1
100	0.0300	20	14.6	12.5
110	0.0431	16	8.4	7.4
115	0.0482	15	6.7	5.8
125	0.0590	15	4.2	3.6
150	0.0828	13	1.4	1.3
175	0.1010	12	0.57	0.51

uncertainty on the signal acceptance includes the uncertainties due to modeling gluon radiation from the initial-state or final-state partons (10%), and the choice of the PDF (4%). The limited size of the leptoquark simulation samples gives a 3% statistical uncertainty. The signal acceptance uncertainty due to the jet energy scale varies from 4% to 26%, and the uncertainty on the luminosity is 6%. The uncertainty on the trigger efficiency is 1%. The theoretical uncertainties on the renormalization and factorization scales are not included here, since we conservatively choose the NLO cross section setting $\mu = 2m_{LQ_1}$ to extract the limits on leptoquark mass. This choice of scale is found to reduce the cross section prediction by 15% relative to $\mu = m_{LQ_1}$ [18].

In the signal region, we expect 118.5 ± 14.5 events from SM processes and observe 124 events. The predicted backgrounds from SM processes are summarized in Table II. In Figure 1 the predicted \cancel{E}_T distribution

TABLE II: The number of expected events from various SM sources in the leptoquark signal region. The first uncertainty is from the limited simulation statistics and the second is from the various systematics.

Source	Events expected
$W(\rightarrow e\nu)+jets$	$6.1 \pm 1.4 \pm 1.5$
$W(\rightarrow \mu\nu)+jets$	$21.7 \pm 2.3 \pm 2.8$
$W(\rightarrow \tau\nu)+jets$	$28.4 \pm 3.8 \pm 4.1$
$Z(\rightarrow \mu\mu)+jets$	$1.1 \pm 0.2 \pm 0.2$
$Z(\rightarrow \tau\tau)+jets$	$0.9 \pm 0.2 \pm 0.2$
$Z(\rightarrow \nu\nu)+jets$	$39.1 \pm 2.8 \pm 3.6$
$t\bar{t}$	$4.3 \pm 0.4 \pm 0.3$
QCD	16.9 ± 6.7
Total Events	118.5 ± 14.5

is compared with the distribution observed in data. No evidence for leptoquark production is observed. We calculate the upper limit at the 95% confidence level (C.L.)

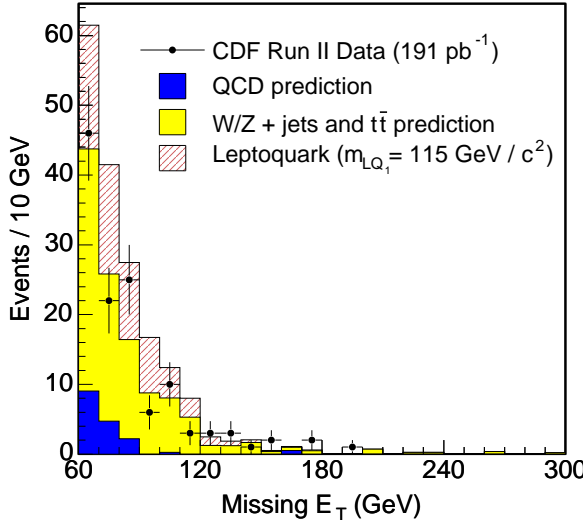


FIG. 1: The \cancel{E}_T distribution in the leptoquark signal region for data (solid points) compared to SM background (shaded histograms). Also shown is the expected distribution arising from leptoquark production and decay at a mass of $115 \text{ GeV}/c^2$ (hatched histogram).

on the pair production cross section times the square of the branching ratio of the leptoquark to a quark and a neutrino using a Bayesian approach [19] with a flat prior for the signal cross section and Gaussian priors for acceptance and background uncertainties. The upper limit on the cross section times $(1 - \beta)^2$ is shown in Figure 2 and is compared with the theoretical cross sections. The theoretical cross sections for scalar leptoquark production have been calculated at NLO using CTEQ5M [17] PDFs.

In conclusion, we performed a search for leptoquarks in the jets and \cancel{E}_T topology using 191 pb^{-1} of CDF Run II data. No evidence for leptoquarks is observed. We set an upper limit on the production cross section at the 95% C.L. Assuming a leptoquark decays into a neutrino and quark with 100% branching ratio, we exclude the mass interval from 78 to $117 \text{ GeV}/c^2$ for first-generation scalar leptoquarks. This extends the previous limit for the first-generation scalar leptoquark of $98 \text{ GeV}/c^2$ [4].

We thank the Fermilab staff and the technical staffs of the participating institutions for their vital contributions. This work was supported by the U.S. Department of Energy and National Science Foundation; the Italian Istituto Nazionale di Fisica Nucleare; the Ministry of Education, Culture, Sports, Science and Technology of Japan; the Natural Sciences and Engineering Research Council of Canada; the National Science Council of the Republic of China; the Swiss National Science Foundation; the A.P. Sloan Foundation; the Bundesministerium für Bildung und Forschung, Germany; the Korean Sci-

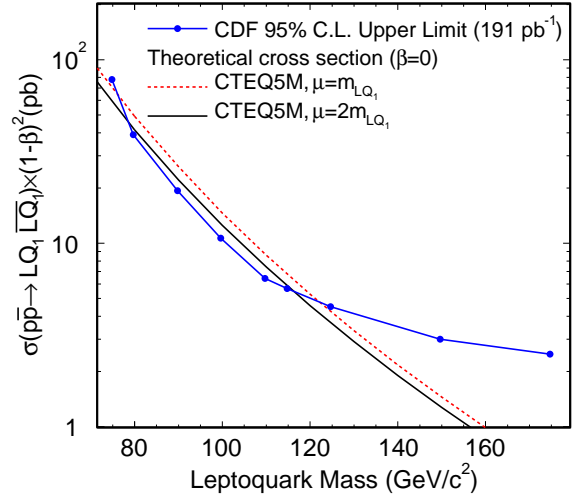


FIG. 2: The upper limit on the cross section times squared branching ratio for scalar leptoquark production in the jets and \cancel{E}_T topology. Also shown is the NLO cross section for $\beta = 0$ for 2 choices of the factorization/renormalization scale: $\mu = m_{LQ_1}$, $\mu = 2 m_{LQ_1}$.

ence and Engineering Foundation and the Korean Research Foundation; the Particle Physics and Astronomy Research Council and the Royal Society, UK; the Russian Foundation for Basic Research; the Comision Interministerial de Ciencia y Tecnologia, Spain; in part by the European Community's Human Potential Programme under contract HPRN-CT-20002, Probe for New Physics.

-
- [1] W. Buchmüller, R. Rückl and D. Wyler, Phys. Lett. B191, 442 (1987) and Erratum B448, 320 (1999).
 - [2] S. Davidson, D. Bailey and B. A. Campbell, Z. Phys. C61, 613 (1994).
 - [3] S. Klimenko, J. Konigsberg and T. Liss, FERMILAB-FN-0741 (2003); D. Acosta *et al.*, Nucl. Instrum. Meth. A494, 57 (2002).
 - [4] V.M. Abazov *et al.* (DØ Collaboration), Phys. Rev. Lett. 88, 191801 (2002).
 - [5] T. Affolder *et al.* (CDF Collaboration), Phys. Rev. Lett. 85, 2056 (2000).
 - [6] D.E. Acosta and S.K. Blessing, Annu. Rev. Nucl. Part. Sci. 49, 389 (1999).
 - [7] CDF Collaboration, FERMILAB-PUB-96/390-E.
 - [8] CDF uses a cylindrical coordinate system in which θ is the polar angle to the proton beam, ϕ is the azimuthal angle about the beam axis, and pseudorapidity is defined as $\eta = -\ln \tan(\theta/2)$. The transverse energy and transverse momentum are defined as $E_T = E \sin \theta$ and $p_T = p \sin \theta$, where E is energy measured in the calorimeter and p is momentum measured by the tracking system. The missing transverse energy vector, \cancel{E}_T , is $-\sum_i E_T^i \mathbf{n}_i$, where \mathbf{n}_i is the unit vector in the azimuthal plane that points from the beamline to the i th calorimeter tower.

- [9] F. Abe *et al.* (CDF Collab.), Phys. Rev. **D45**, 1448 (1992).
- [10] The physical calorimeter towers are organized into larger trigger towers, covering approximately 0.26 in $\Delta\phi$ and 0.22 in $\Delta\eta$.
- [11] F_{em} is the ratio of the energy measured by the electromagnetic calorimeter to the total energy contained in jets of cone radius $\Delta R = 0.4$ with $E_T > 10$ GeV and $|\eta| < 3.6$. F_{ch} is the fraction of the jet energy carried by measured charged-particle tracks ($p_T > 0.5$ GeV/c) averaged over the central jets with $|\eta| < 0.9$. These variables are similar to ones used in T. Affolder *et al.* (CDF Collaboration), Phys. Rev. Lett. **88**, 041801 (2002).
- [12] M.L. Mangano *et al.*, JHEP **07**, 001 (2003). We use version 1.2.
- [13] G. Corcella *et al.*, JHEP **01**, 010 (2001); hep-ph/0210213.
- We use version 6.4a.
- [14] D. Acosta *et al.* (CDF Collaboration), Phys. Rev. Lett. **93**, 142001 (2004).
- [15] T. Sjostrand, P. Eden, C. Friberg, L. Lonnblad, G. Miu, S. Mrenna and E. Norrbin, Computer Physics Commun. **135**, 238 (2001), version 6.203.
- [16] T. Affolder *et al.* (CDF Collaboration), Phys. Rev. D **65** 092002 (2002).
- [17] H. L. Lai *et al.* (CTEQ Collaboration), Eur. Phys. J. **C12** 375 (2000).
- [18] M. Krämer, T. Plehn, M. Spira and P.M. Zerwas, Phys. Rev. Lett. **79**, 341 (1997).
- [19] J. Conway, CERN 2000-005, 247 (2000). The posterior probability density is rendered normalizable by introducing a reasonably large cutoff.